

## MAGNETIC PROPERTIES AND EXCHANGE BIAS BEHAVIOR OF POLY(4-(OCTYLOXY) PHENYL-5-(THIOPHEN-3-YL)-2-NAPHTHOATE): INSIGHTS FROM TEMPERATURE-DEPENDENT MAGNETIZATION AND EPR SPECTROSCOPY

Sankaran Esakki Muthu<sup>1\*</sup>, Baburao Gaddala<sup>2</sup>, Ananthkrishnan<sup>3</sup>, Somanathan<sup>3</sup>, Mandal<sup>3</sup>,  
Karthik Kannan<sup>4</sup>, Nirmal Kumar Balaraman<sup>5</sup> and Sonachalam Arumugam<sup>6</sup>

<sup>1</sup>Centre for Material Science, Department of Physics, Faculty of Arts Science Commerce and Humanities, Karpagam Academy of Higher Education, Coimbatore -641021, India  
<sup>2</sup>Department of Chemical Engineering, School of Studies of Engineering and Technology, Guru Ghasidas Vishwavidyalaya (A Central University), Koni, Bilaspur, Chhattisgarh-495009, India  
<sup>3</sup>Polymer Laboratory, Central Leather Research Institute, Adyar, Chennai 600020, India  
<sup>4</sup>Department of Mechanical Engineering, Advanced Institute of Manufacturing with High-Tech Innovations, National Chung Cheng University, Chia-Yi, 621301, Taiwan  
<sup>5</sup>Inframark LLC/MR Systems LLC, Georgia, GA 30093, USA  
<sup>6</sup>Centre for High Pressure Research, Bharathidasan University, Tiruchirappalli -620024, Tamil Nadu, India

(Received July 14, 2024; Revised December 20, 2024; Accepted December 23, 2024)

**ABSTRACT.** The polymer POPTN was investigated to elucidate its magnetic and optoelectronic properties, with particular emphasis on charge carrier mobility, dichroic behaviour, and magnetic interactions. Electron paramagnetic resonance (EPR) studies confirmed delocalization over the naphthalene side chains, contributing to the observed paramagnetic behaviour at room temperature. Temperature-dependent magnetic studies revealed paramagnetic behaviour at higher temperatures transitioning to weak ferromagnetism below 10 K. Curie-Weiss analysis indicated antiferromagnetic (AFM) coupling with a paramagnetic Curie temperature ( $\theta_p$ ) of -203 K. Exchange bias (EB) measurements demonstrated a significant hysteresis loop shift at 2 K, diminishing with increasing temperature and vanishing near 20 K. The maximum exchange bias field ( $H_E$ ) was observed to be 133 Oe at 2 K, attributed to the coexistence of ferromagnetic (FM) and AFM interactions. The interplay of AFM and FM coupling, along with  $\pi$ - $\pi$  stacking facilitated by the naphthyl moiety, influenced the magnetic properties and anisotropy.

**KEY WORDS:** Antiferromagnetism (AFM), Ferromagnetism (FM), Exchange bias, Paramagnetism, Electron paramagnetic resonance (EPR) spectroscopy, Temperature dependence of magnetization

### INTRODUCTION

Organic electronic devices based on polymers, where the elastic current is controlled by electron spin to improve performance, serve as a basis for several technologies. The utilisation of polymers and organic materials in spintronic devices presents several benefits, such as improved functionality, simplified production, and economic viability. Organic materials are perfect for investigating spin quantum device concepts because of their lengthy spin coherence times, which are caused by the weak spin-orbit interaction between low-atomic-number atoms, such as carbon. In the realm of spintronics, extensions of spin valves based on magnetic semiconductors and associated spin light-emitting diodes have demonstrated potential. Conducting polymers are appropriate for a wide range of applications because of their diverse optical, electrical, and electronic properties [1, 2]. Among the difficulties that polymers assist with include inadequate spin injection at surfaces, low sensitivity and low Curie temperature. Less research has been done

---

\*Corresponding authors. E-mail: sanrajson@yahoo.com

This work is licensed under the Creative Commons Attribution 4.0 International License

on polymers' magnetic properties, though. Generally speaking, unpaired electrons' intrinsic spin is what gives molecules their magnetic [3]. Magnetic order can be produced by these spins aligning themselves either parallel or antiparallel through mutual magnetic contact. When unpaired electrons in the same molecules have the same spin orientation, ferromagnetism results. Cooperative spin orientation among molecules is necessary to design a material with macroscopic magnetism [2]. The magnetic properties of polymers are also influenced by the orientation of their functional groups in the bulk. In order to align spins in the direction of an external magnetic field and achieve ferromagnetic spin coupling, the substitution pattern and connection are essential. Under certain circumstances, certain conjugated polymers have demonstrated magnetic characteristics. Doped polypyrroles, polyanilines, Potential candidates with magnetic characteristics include functionalized polyacetylenes and polyalkylthiophenes [4]. The magnetic characteristics of polythiophene nematogen (poly 4-(octyloxy) phenyl-5-(thiophen-3-yl)-2-naphthoate) (POPTN), which has naphthalene in the side chain and ester connecting groups, are reported in this article. It also provides information on POPTN's exchange bias (EB) behaviour. The AFM and FM system's hysteresis loops are shifted down the field axis by the exchange anisotropy that is formed after cooling in the presence of an applied magnetic field at the interface between ferromagnetic (FM) and antiferromagnetic (AFM) materials. This phenomenon is linked to the observed events. Small oxide particles, heterogeneous materials, nanostructures, and multilayer films have all been shown to exhibit this behavior [5-11]. Additionally, materials possessing a spin glass phase exhibit the EB phenomena [12-14]. A 133 Oe tiny exchange bias field (HE) was seen at a temperature of 2K for POPTN

## EXPERIMENTAL

POPTN was synthesized by a multi stage process using Suzuki coupling. The OPTN monomer was synthesized by a 4-stage synthetic procedure involving Suzuki coupling. 4-Hydroxy methyl benzoate was treated with the corresponding 1-bromo alkanes to get 4-alkoxy methyl benzoate. The 4-alkoxy methyl benzoate was again hydrolyzed to get 4-alkoxy benzoic acid which was coupled with 6-bromonaphthol using Slater esterification to get the bromo precursor. The above precursor was again coupled with thiophene-3-boronic acid using Suzuki coupling to get the monomer. The OPTN monomer was polymerized using anhydrous  $\text{FeCl}_3$  to get the polymer which was washed with methanol and purified using Soxhlet extraction with methanol to get undoped POPTN. The entire process is shown in Figure 1. Computational study of the molecule was done using Gaussian 03 (revision E 0.1) program packages [15] DFT/B3LYP/6-31G\*\*. The EPR spectrum of the compound was studied using X band CW EPR facility with variable temperature capability (EMXC 102.1). The absorption spectra of the thin films were studied using Cary 50Bio UV-Vis spectrophotometer. Diodes were fabricated using the polymer as semiconducting layer and Indium tin oxide and aluminum as electrodes. Charge carrier mobility of the semiconductor was studied using the above diodes by under contact limited conditions. A vibrating sample magnetometer (VSM) module from Quantum Design, USA, part of the physical property measurement system (PPMS-9T), was used to measure magnetization. Initially, in the absence of a magnetic field, the sample was cooled to the lowest temperature, and data was acquired during warming while applying a magnetic field of 10 mT (referred to as zero-field cooling, or ZFC). Subsequently, data in the temperature range of 300–2 K was collected during cooling without removing the applied magnetic field (referred to as field cooling, or FC). Additionally, magnetization as a function of the magnetic field was measured at low temperatures, with fields applied up to 1 T.

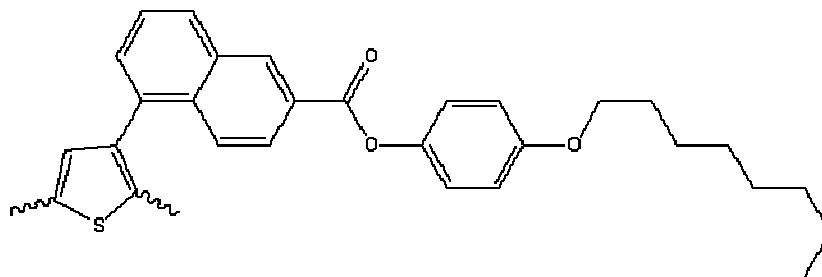


Figure 1. Structure of polythiophene nematogen containing naphthalene in the side chain with ester linking groups (poly 4-(octyloxy) phenyl-5-(thiophen-3-yl)-2-naphthoate) (POPTN).

## RESULTS AND DISCUSSION

Basic properties of the polymer were studied to comprehend the magnetic properties. Charge carrier mobility of POPTN in the device is  $2.42 \times 10^{-7} \text{ cm}^2 \text{ v}^{-1} \text{ s}^{-1}$ , and the mobility of the POPTN in undoped state is comparable to that of undoped region regular poly 3-n-hexyl thiophene [1]. POPTN shows high absorption and the dichroic ratios calculated on the basis of different angles (Table 1). The above results show that the polymers have self-organization and preferential orientation. The dichroic ratio observed in POPTN thin films serves as a crucial measure of the degree of molecular alignment and self-organization within the material. A high dichroic ratio suggests that the polymer chains are preferentially oriented, leading to enhanced optical anisotropy, which is critical for tuning the material's optical and electronic properties. This orientation and self-organization influence the material's performance in various optoelectronic and magnetic applications, providing opportunities for device optimization based on the controlled alignment of POPTN molecules. The delocalization of valence electron density over liquid crystalline moiety (side chain containing naphthalene ring) causes hyper fine splitting. The observed hyperfine splitting indicates that the unpaired electron density is localized near certain atomic nuclei. This suggests a lack of complete delocalization of spins along the polymer backbone, which may result from the localized electronic states due to structural irregularities and weak  $\pi$ -conjugation or disruptions in the polymer's electronic structure. The EPR spectra with  $g$  value 1.9980 (Figure 2) of POPTN shows a broad signal suggesting a presence of hyperfine structure, which in turn signifies the delocalization over naphthalene moiety. This kind of delocalization is also shown by the distribution of Highest Occupied Molecular Orbital (HOMO) calculated by DFT/B3LYP/-631G\*\* calculations (Figure 3). The intensity of the EPR signals of POPTN polymer at room temperature shows the presence of unpaired electrons, which indicates the paramagnetic behavior at room temperature. It is noteworthy to observe that in the instance of POPTN, the optimized geometry shows some directional nature of orientation of naphthyl moiety (Figure 4). The orientation of the EPR active naphthyl moieties can show some distinct properties with temperature and under magnetic field. The above results confirm that the POPTN shows paramagnetic properties at room temperature. Further the naphthyl moiety, being an extended aromatic system, contributes to  $\pi$ -conjugation along the polymer backbone. Its orientation affects the overlap of  $\pi$ -orbitals, thereby influencing the delocalization of electronic spins and the overall magnetic moment and response to an applied field. Favorable orientations promote  $\pi$ - $\pi$  stacking between adjacent chains, which strengthens intermolecular magnetic coupling. Enhanced  $\pi$ - $\pi$  stacking may increase exchange interactions, leading to cooperative magnetic phenomena, such as ferromagnetic or antiferromagnetic ordering at low temperature below 10 K which can be seen in Figure 5.

Table 1. Showing the absorption dichroic ratio of POPTN thin films.

Wavelength range (nm)	Dichroic ratio	
	0/90	180/270
233	0.78	1.22
266	0.96	1.10
340	0.89	1.03
361	1.02	1.24

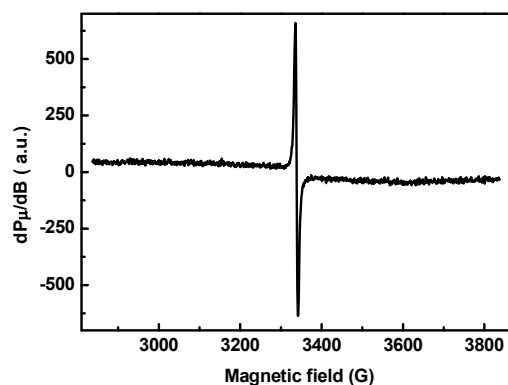


Figure 2. The EPR spectra of POPTN.

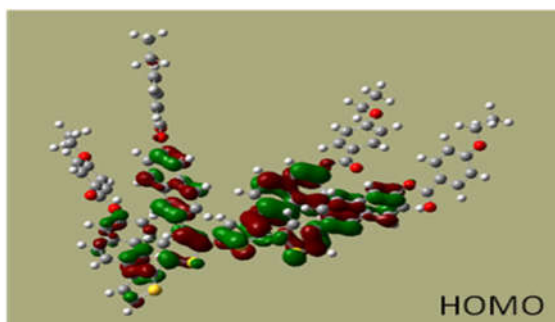


Figure 3. Molecular orbital distribution of POPTN using DFT/B3LYP 6-31G\*\*.

To further study the magnetic properties of POPTN, it was measured how temperature affected magnetism for POPTN in 10 mT magnetic field on ZFC and FC are shown in Figure. 5. The sample shows a paramagnetic behavior at higher temperature and show a weak ferromagnetism below 10 K. The inverse susceptibility measured shows that the magnetization is linear in the higher temperature portion as a function of temperature and deviates with low temperature. The linear portion at higher temperatures follows the Curie-Weiss law and the observed paramagnetic Curie temperature  $\theta_p = -203$  K revealing the presence of antiferromagnetic coupling in the sample. The observed low-temperature behavior may imply that POPTN has localized magnetic moments, potentially due to unpaired electrons or structural features enabling magnetic interactions. This low-temperature nonlinearity likely reflects the influence of weak, possibly disordered magnetic interactions or spin dynamics in POPTN. At low temperature the observed irreversibility between

ZFC and FC curves indicates ferromagnetic and antiferromagnetic interaction coexisting in the sample. The pinning of FM and AFM at low temperature leads to the exchange bias behavior in the sample. To confirm the AFM in the low temperature a Curie equation,  $H/M = C/T^\gamma$  is displayed as a log-log plot of  $H/M$  vs.  $T$  in the inset of Figure 5. For behaviour below 10 K, the straight-line representing  $H/M$  vs.  $T$  shows the existence of a nature of magnetic material. The typical  $\gamma$  value for paramagnetic particles or super paramagnetic material is 1. The obtained gamma value of 0.6826, which is less than 1 indicates that the antiferromagnetic interaction exists in the sample. The Curie equation for the confirmation of the magnetic property at low temperature is previously used by Bhowmik *et al.* [16] in the pure magnetic system in nature and by Sambandam *et al.* [17] in the diluted magnetic system. The AFM observed in POPTN is also confirmed by the obtained EPR results.

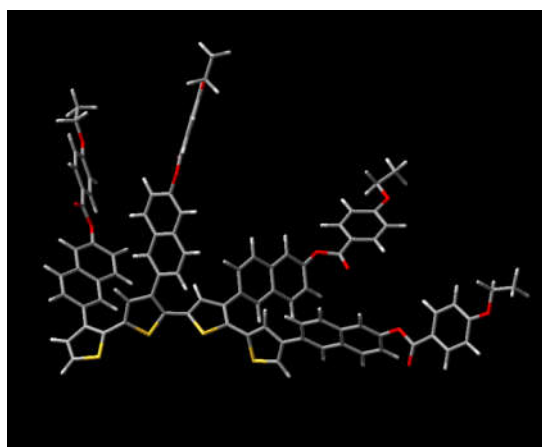


Figure 4. Optimized geometries of POPTN (tetramer).

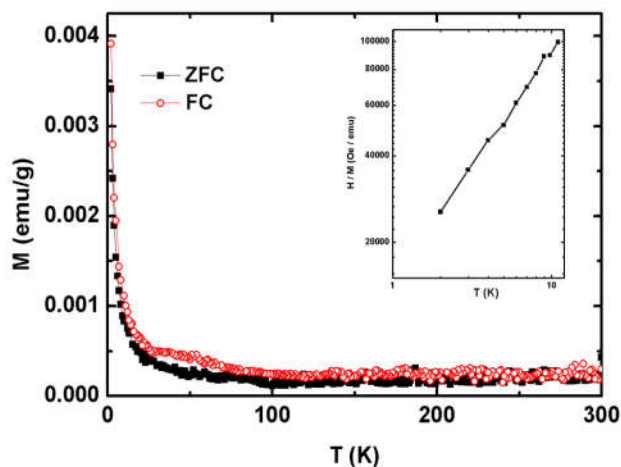


Figure 5. ZFC and FC thermo magnetic curve for POPTN at a field of 10 mT.

In order to study the exchange bias, investigations were done on EB with various temperature for POPTN in the temperature interval 2, 5, 10, 15, 20, 25, 30 and 50 K, and the standard FC curves for POPTN are shown in Figure. 6. By chilling the sample in a field of 10 kOe, the FC loop was measured. Curves in the low field regions are displayed to improve the visibility of the loop shift. Figure 6 clearly shows that at 2 K temperature, the hysteresis loops strongly shifted to the negative field from the origin, indicating the presence of EB in the sample. Such behaviour indicates the presence of AFM-FM interactions in the system at low temperatures, and the hysteresis's loop shift, diminishes with increasing temperature. Around 20 K, the field shift nearly vanishes and the loop becomes symmetric.

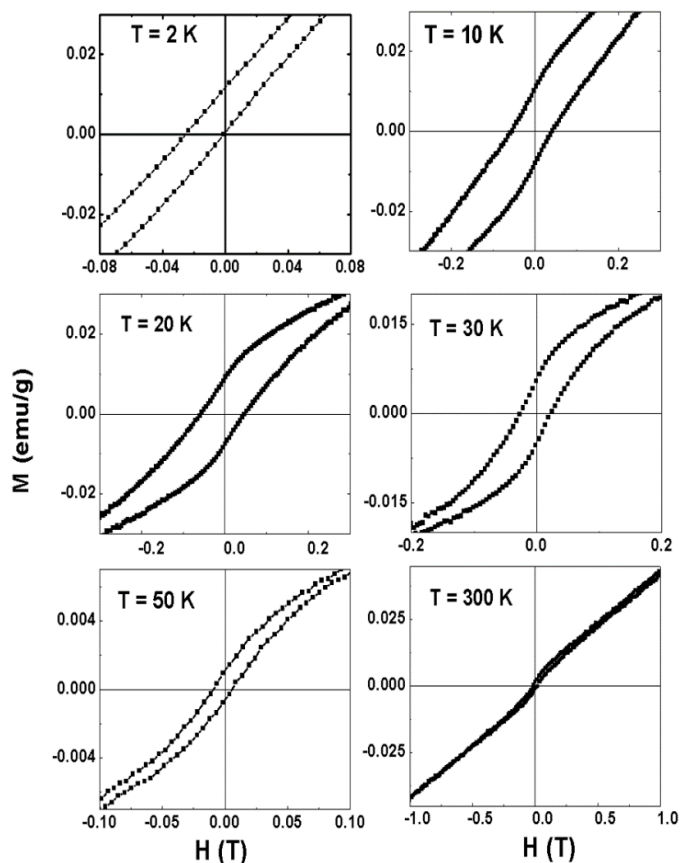


Figure 6. FC magnetic hysteresis loop measured at various temperatures for POPTN. Loop shift decreases with temperature.

The M-H curve at high temperature (300 K) shows a clear paramagnetic contribution. This observed paramagnetic behavior at high temperature is confirmed by the EPR experiment. Coercivity ( $H_C$ ) and EB field ( $H_E$ ) values are evaluated from the hysteresis loops of POPTN and exhibited at different temperatures (Figure 7).  $H_E = -(H_1 + H_2)/2$  and  $H_C = |H_1 - H_2|/2$ , respectively, were used to compute the values of  $H_E$  and  $H_C$ , where  $H_1$  stands for the negative field and the positive field represented by  $H_2$  at which the magnetization equals zero. Figure 7 shows that  $H_E$

reduces proportionately to temperature rise and eventually vanishes about  $T_C$ , indicating that the EB phenomenon is real for temperatures below  $T_C$ . This is explained by the fact that when temperature rises, FM-AFM coupling becomes weaker. Conversely, after reaching a maximum value,  $H_C$  starts to decrease with temperature instead of increasing initially. And the anisotropy of AFM is known to diminish as temperature rises. The value of  $H_E$  observed in 2 K is 133 Oe. Thus, the EB observed in POPTN is a new material system which can be used in spin electronic devices.

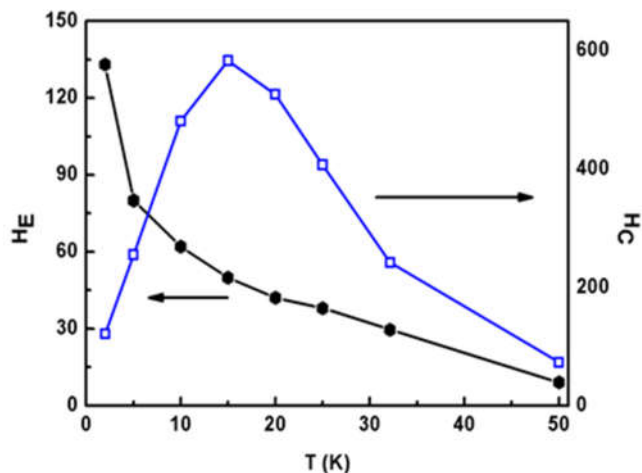


Figure 7. Variation of EB field ( $H_E$ ) and coercivity ( $H_C$ ) with temperature for POPTN.

## CONCLUSION

This study highlights the magnetic properties of POPTN, making it suitable for spintronic applications. At room temperature, POPTN shows paramagnetic behavior, while at low temperatures, it exhibits both ferromagnetic and antiferromagnetic interactions. The naphthalene side chains enhance spin delocalization and magnetic coupling. EPR spectra confirm unpaired electron spins and partial delocalization. Temperature affects the material's magnetic properties, with exchange bias and coercivity observed at low temperatures. The weak spin-orbit interaction ensures long spin coherence times. POPTN's scalable synthesis makes it practical for flexible, large-scale applications. Its tunable magnetic properties address key challenges in spintronics. Molecular design allows POPTN to bridge the gap between organic materials and advanced spintronic technologies. POPTN provides a promising platform for next-generation spintronic devices.

## REFERENCES

1. Skotheim, T.A.; Elsenbaumer, R.S.; Reynolds, J.R. *Handbook of Conducting Polymers*, 2nd ed., Marcel Dekker: New York; **1998**.
2. Epstein, A.J., Prigodin, V.N., U.S. Patent US6, 621,100 B2, dt. 16.9, **2003**.
3. Vandeleene, S.; Jivanescu, M.; Stesmans, A.; Cuppens, J.; Van Beal, M.J.; Yamada, H.; Sato, N.; Verbiest, T.; Koeckelberghs, G. Magnetic properties of substituted poly(thiophene)s in their neutral state. *Macromol.* **2010**, 43, 2910-2915.
4. Vandeleene, S.; Jivanescu, M.; Stesmans, A.; Cuppens, J.; Margriet, J.; Van Beal, M.J.;

- Verbiest, T.; Koeckelberghs, G. Influence of the supramolecular organization on the magnetic properties of poly(3-alkylthiophene)s in their neutral state. *Macromol.* **2011**, *44*, 4911-4919.
5. Sugumar, M.; Bharathi, S.; Sampath, V.; Sundramurthy, V.P.; Selvaraju, M.; Kadaikunnan, S.; Khaled, J.M. Biosorption of Pb(II) ions through nanostructured teff straw based magnetized activated biocarbon: aspects on modeling, optimization, and kinetics. *Global NEST J.* **2024**, *26*, 04679.
  6. Mohanasundaram, S.; Geetha, S.; Nagajothi, R.; Sundramurthy, V.P.; Vijayakumar, J.; Alharbi, N.; Thiruvengadam, M. Evaluation of anti-corrosion potential of datura metal plant extract on mild steel upon sulphuric acid exposure. *Can. Metall. Q.* **2024**, 1-14, DOI: <https://doi.org/10.1080/00084433.2024.2310352>.
  7. Kumar, D.D.; Balamurugan, A.; Suresh, K.C.; Kumar, R.S.; Jayanthi, N.; Ramakrishnan, T.; Ahammad, S.K.H.; Mayakannan, S.; Prabhu, S.V. Study of microstructure and wear resistance of AA5052/B4C nanocomposites as a function of volume fraction reinforcement to particle size ratio by ANN. *J. Chem.* **2023**, 2023, 2554098.
  8. Stamps R.L. Mechanisms for exchange bias. *J. Phys. D: Appl. Phys. D* **2000**, *33*, R247.
  9. Qian, T.; Li, G.; Zhang, T.; Zhou, T.F.; Xiang, X.Q.; Kang, X.W.; Li, X.G. Exchange bias tuned by cooling field in phase separated  $Y_{0.2}Ca_{0.8}MnO_3$ . *Appl. Phys. Lett.* **2007**, *90*, 012503.
  10. Fraune, M.; Rüdiger, U.; Güntherodt, G.; Cardoso, S.; Freitas, P.; Size dependence of the exchange bias field in NiO/Ni nanostructures. *Appl. Phys. Lett.* **2000**, *77*, 3815-3817.
  11. Gruyters, M. Spin-glass-like behavior in CoO nanoparticles and the origin of exchange bias in layered CoO/ferromagnet structures. *Phys. Rev. Lett.* **2005**, *95*, 077204.
  12. Kodama, R.H.; Makhlof, S.A.; Berkowitz, A.E. Inite size effects in antiferromagnetic NiO Nanoparticles. *Phys.Rev. Lett.* **1997**, *79*, 1393-1396.
  13. Merzouki, Z.E.; Rkhioui, N-D.; Benhsin, E.H.; Cherraj, M. The magnetic characteristics and electronic configuration of gan compound modified by individual impurities (Fe And Ni). *Bull. Chem. Soc. Ethiop.* **2024**, *38*, 1861-1868.
  14. Tesfaw, B.; Chekol, F.; Mehretie, S.; Admassie, S. Adsorption of Pb(II) ions from aqueous solution using lignin from *Hagenia abyssinica*. *Bull. Chem. Soc. Ethiop.* **2016**, *30*, 473-484.
  15. Frisch, M.J.; Trucks, G.W.; Schlegel, H.B. *Gaussian 03, revision E. 01*, Gaussian Inc.: Wallingford CT; **2004**.
  16. Bhowmik, R.N.; Nagarajan, R.; Ranganathan, R. Magnetic enhancement in antiferromagnetic nanoparticle of  $CoRh_2O_4$ . *Phys. Rev. B* **2004**, *69*, 054430.
  17. Sambandam, B.; Rajendran, N.; Kanagaraj, M.; Arumugam, S.; Manoharan, P.T. Switching on antiferromagnetic coupled superparamagnetism by annealing ferromagnetic Mn/CdS nanoparticles. *J. Phys.Chem .C* **2011**, *115*, 11413-11419.